



## Full Length Article

Green synthesis and detailed characterization of selenium nanoparticles derived from *Alangium salviifolium* (L.f) Wangerin

Karunya Saravanan<sup>a</sup>, Manivannan Madhaiyan<sup>b</sup>, Prabu Periyasamy<sup>b</sup>, Prasath Manivannan<sup>c</sup>, Alpaslan Bayrakdar<sup>d</sup>, Dr. V. Balakrishnan<sup>a,\*</sup>

<sup>a</sup> PG & Research Department of Botany, Aringar Anna Government Arts College, Namakkal 637 002, Tamil Nadu, India

<sup>b</sup> Department of Biotechnology, Periyar University Centre for Post Graduate and Research Studies, Dharmapuri 635205 Tamil Nadu, India

<sup>c</sup> Department of Physics, Periyar University Centre for Post Graduate and Research Studies, Dharmapuri 635205 Tamil Nadu, India

<sup>d</sup> Vocational school of Higher education for Health services, Igdir University, Turkiye

## ARTICLE INFO

## Keywords:

Se NPs  
Bio synthesis  
*A. salviifolium*  
Green synthesis  
Surface plasmon resonance

## ABSTRACT

In recent years, the environmentally sustainable synthesis of selenium nanoparticles (Se NPs) has garnered significant interest owing to its prospective applications in medicine, electronics, and environmental remediation. This work investigates the eco-friendly synthesis of Se NPs using extracts from *Alangium salviifolium* leaves and fruits, emphasizing the optimization of the extraction method to increase the output of phytochemicals that promote the reduction of selenium ions into nanoparticles. The characterization of the synthesized Se NPs was conducted utilizing sophisticated analytical techniques to clarify their structural, morphological, and compositional attributes. UV-Vis spectroscopy validated the effective synthesis of Se NPs via a characteristic surface plasmon resonance peak. The FTIR study elucidated the functional groups in the extracts and their interactions with selenium throughout the reduction process. XRD analysis demonstrated the crystalline structure of the produced nanoparticles, with peaks aligned to distinct selenium phases, so validating their effective synthesis. FESEM integrated with EDS offered detailed morphological insights and elemental composition analysis, demonstrating uniform distribution and size consistency among the nanoparticles. Elemental mapping further corroborated the presence of selenium within the synthesized structures. Additionally, HR-TEM combined with SAED provided atomic-level insights into the crystallinity and size distribution of Se NPs, revealing their potential for various applications. The synthesized nanoparticles exhibited remarkable stability and biocompatibility, suggesting promising prospects for biomedical applications. This study not only highlights an effective green synthesis route for Se NPs but also underscores the importance of utilizing natural resources in nanomaterial production. The findings contribute significantly to nanotechnology by providing a sustainable approach to nanoparticle synthesis while paving the way for future research into their functional applications across diverse sectors.

## 1. Introduction

The progress in nanotechnology has transformed the field of biomedicine by leveraging the distinctive characteristics of nanoparticles (NPs) for various applications, including diagnostics and targeted drug delivery, Se NPs are particularly essential since they serve as critical trace elements vital for the well-being of humans and animals. Their growth is crucial in battling harmful germs [1]. Selenium was formerly regarded as a toxic material until its identification as an essential trace element by Schwarz and Foltz in 1957, crucial for the

health of both plants and animals [2]. Nano-ultrafine particles of the indispensable micronutrient selenium have exhibited remarkable potential in the biomedical sector. The chemical symbol for selenium, which was discovered by Jons Jacob Berzelius in 1817, is Se, and its atomic weight is 78.963 Da [3]. Amorphous selenium micronutrient stabilizes most effectively when it transitions into its hexagonal crystalline structure, which can exhibit various shapes, including a spherical form, similar to that of selenium dioxide nanoparticles [4]. *Alangium salviifolium* is a flowering plant species within the cornaceae family. This blooming plant is recognized for its many medical characteristics and is

\* Corresponding author.

E-mail address: [palanivbalu@gmail.com](mailto:palanivbalu@gmail.com) (V. Balakrishnan).

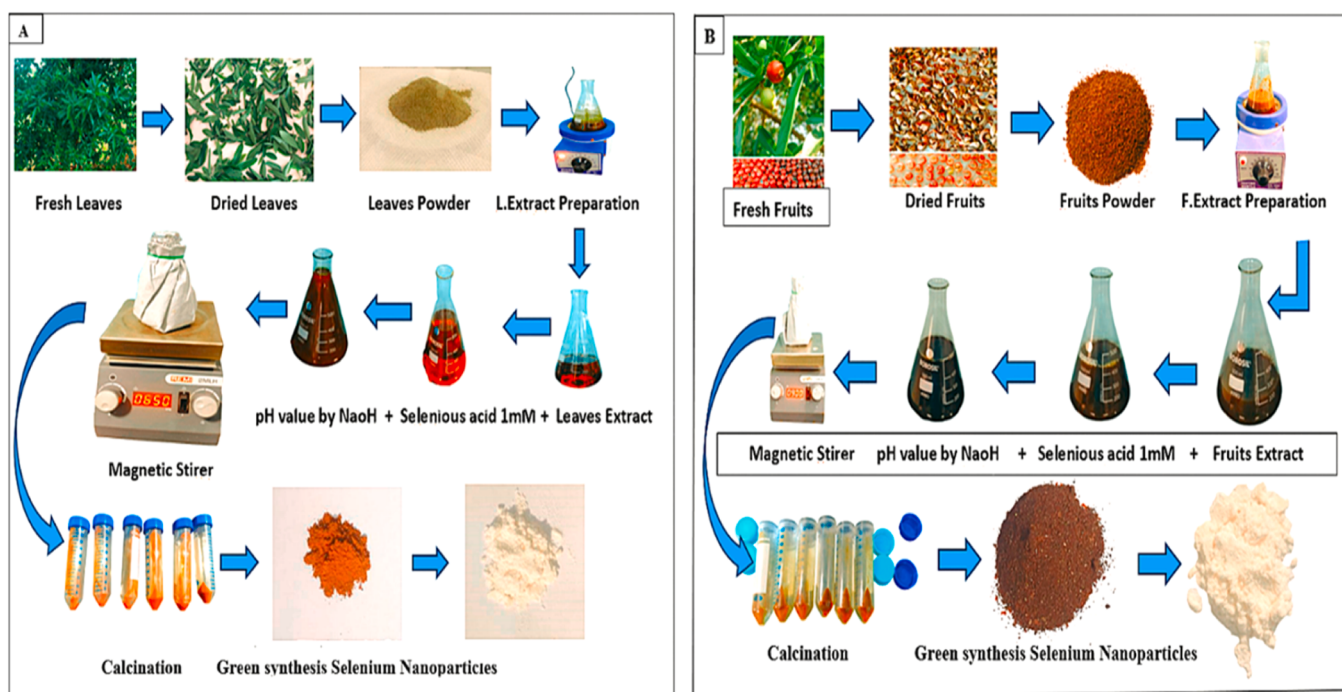


Fig. 1. a. Schematic representation of *Alangium salviifolium* leaves green synthesis Se NPs. b. *Alangium salviifolium* fruits green synthesis Se NPs.

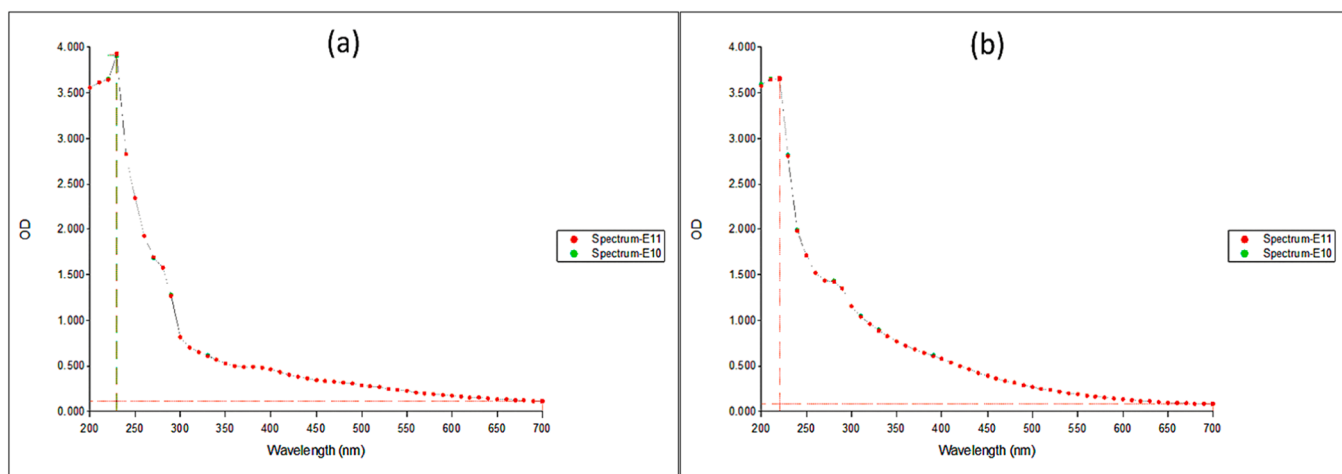
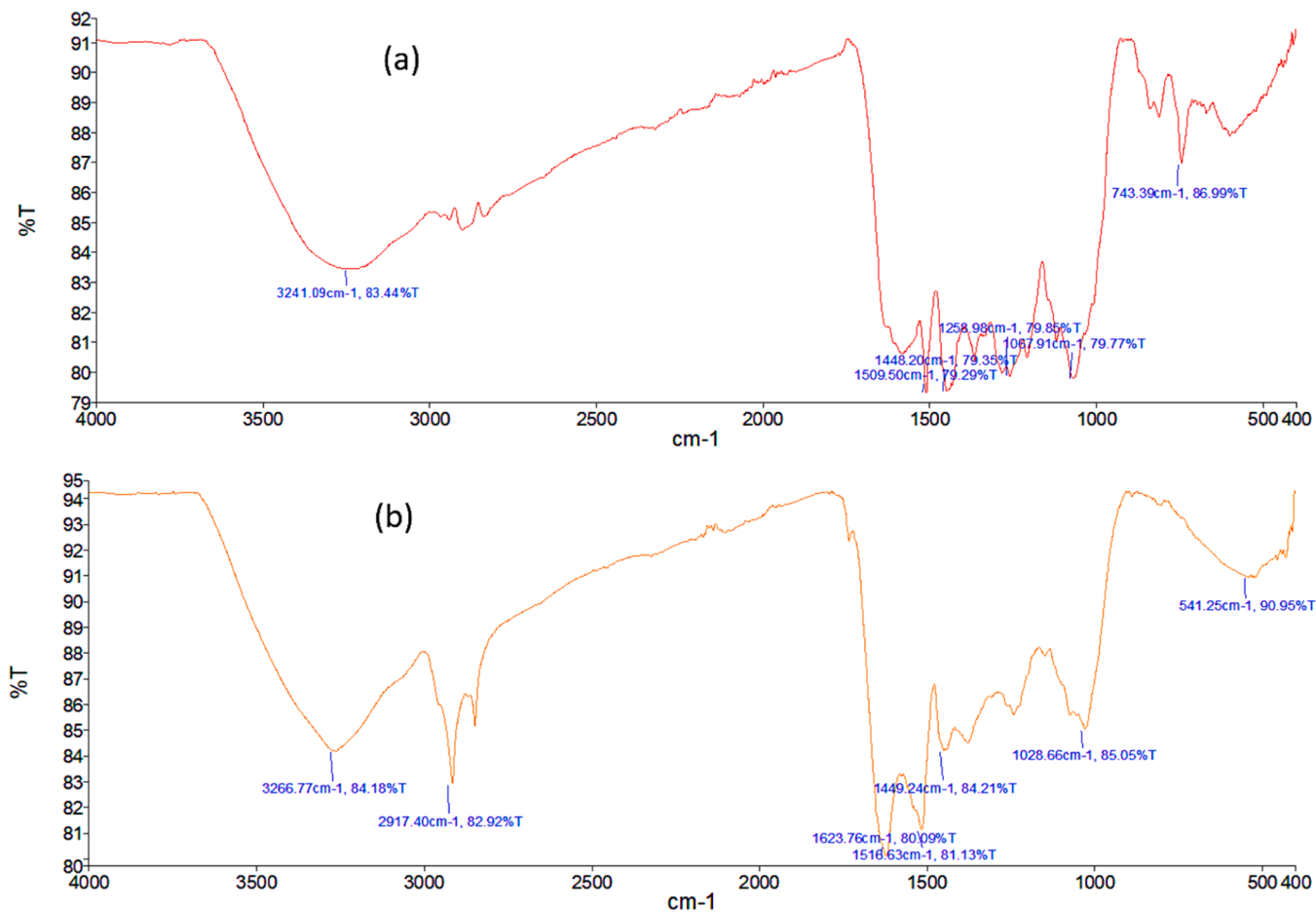


Fig. 2. a. *A. salviifolium* leaf extract using green synthesis Se NPs UV–Visible Spectroscopy. b. *A. salviifolium* fruit extract using green synthesis Se NPs UV–Visible Spectroscopy.

extensively used to alleviate illnesses such as rheumatism, cancer, and diabetes. Additionally, it contributes to maintaining burning sensation, haemorrhage, enhancing constipation and mitigating the effects of hypertension, epilepsy and ulcer [5,6]. Over a 35-day treatment period, the manufacture of silver nanocomposites utilizing garlic extract has demonstrated efficacy in lowering toxicity, exhibiting minimal side effects, and enhancing sperm health in diabetic mice. This method offers intriguing therapeutic implications for diabetes-related reproductive disorders and is both efficient and economical [7]. Furthermore, the environmentally friendly manufacturing of selenium nanoparticles (Se NPs) utilizing *Withania somnifera* root extract was studied. According to a comet assay, these nanoparticles showed protective benefits against diabetes-induced DNA damage and noteworthy structural, morphological, and optical characteristics [8]. Using reducing agents like sodium borohydride or ascorbic acid, the chemical reduction method is a popular technique for creating selenium nanoparticles (Se NPs) from

precursors like sodium selenite or selenate. This method is perfect for both large-scale production and experimental research because it effectively converts selenium ions into elemental selenium, allowing precise control of reaction conditions. It is preferred in fields including environmental science, agriculture, and healthcare because of its capacity to produce pure and stable Se NPs [9]. Utilizing biological resources such as plants and microbes, the environmentally friendly production of nanoparticles provides a sustainable substitute for conventional techniques. By using less energy and harmful chemicals, this method improves the biocompatibility of nanoparticles for use in environmental and medicinal applications [10]. Since bacterial culture necessitates specific methods, knowledge, and equipment in addition to greater maintenance expenses, employing plant extracts for nanoparticle synthesis is more economical than using bacteria or fungi. Plant-derived extraction techniques provide a cost-effective, environmentally friendly, one-step, and green method that decreases solvent



**Fig. 3.** **a.** *A. salviifolium* leaves extract using green synthesis Se NPs characterized by FT-IR. **b.** *A. salviifolium* fruits extract using green synthesis Se NPs characterized by FT-IR.

**Table 1**

FTIR peak values and functional groups in synthesized Se NPs using aqueous leaf extract in *A. salviifolium*.

S. No	Wavenumber (cm <sup>-1</sup> )	Intensity	Bond Responsible	Functional Groups
1	743.39	Strong	C—H bending	Aromatic C—H
2	106.79	Weak	C—H bending	Aliphatic compounds
3	1258.98	Strong	C—O stretching	Alcohols, Ethers
4	1448.20	Medium	C—H bending	Aliphatic Compounds
5	1509.50	Medium	C=C stretching	Aromatic Compounds
6	3241.09	Medium	O—H stretch	Alcohols, Phenols

usage and speeds up response times [11]. The plant extracts contain various compounds, including phenolic acids, flavonoids, and alkaloids, which serve as reducing and stabilizing agents in the synthesis of biocompatible selenium nanoparticles (Se NPs). These secondary metabolites enhance the effectiveness of Se NP production [12]. Our study's novelty lies in the use of a specific plant material *A. salviifolium* (leaves and fruits) for Se NPs synthesis, coupled with an extensive array of characterization techniques (UVVis, FTIR, XRD, FESEM-EDS, and HRTEM-SAED). This comprehensive approach provides a deeper understanding of the morphology, composition, and structure of the synthesized Se NPs, contributing to the growing body of knowledge on eco-friendly nanoparticle synthesis methods. The goal of this research is to create a sustainable and effective process for the green production

**Table 2**

FTIR peak values and functional groups in synthesized Se NPs using aqueous fruits extract in *A. salviifolium*.

S. No	Wavenumber (cm <sup>-1</sup> )	Intensity	Bond Responsible	Functional Groups
1	541.25	Weak	C—X bending	Halides (C—Cl, C—Br)
2	1028.66	Strong	C—O stretching	Alcohols, Ethers
3	1449.24	Medium	C—H bending	Aliphatic Compounds
4	1516.63	Medium	C=C stretching	Aromatic Compounds
5	1623.76	Medium	C=C stretching	Aromatic Compounds
6	2917.40	Strong	C—H stretching	Aliphatic Compounds
7	3266.77	Strong	O—H stretch	Alcohols, Phenols

of selenium nanoparticles (SeNPs) by employing plant extracts as organic stabilizing and reducing agents. Advanced methods like FESEM, EDS, and FTIR will be used to characterize the produced nanoparticles and examine their structural and functional characteristics. The elemental distribution will be seen and surface coatings will be analyzed using UVVisible spectroscopy, HR-TEM, and SAED patterns. Additionally, for thorough characterization to comprehend the crystalline structure and functional groups present in the SeNPs, XRD and FTIR investigations will be carried out. By utilizing plant-based techniques for nanoparticle manufacturing and investigating their possible uses, this study aims to environmentally friendly nanotechnology.

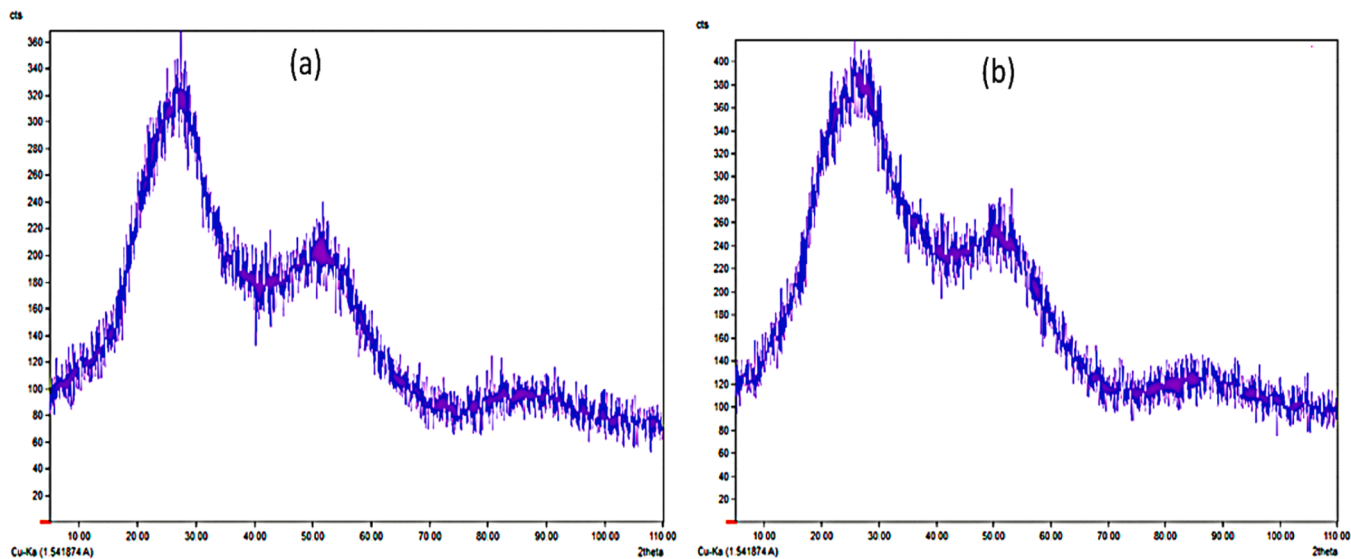


**Fig. 4.** *A. salviifolium* leaf extract using green synthesis Se NPs characterized by X-ray diffractometer. **b** *A. salviifolium* fruit extract using green synthesis Se NPs characterized by X-ray diffractometer.

## 2. Experimental

### 2.1. Plant collection and materials

The healthy leaves and fruit of *A. salviifolium* were collected in Kadappalli, Namakkal District, Tamil Nadu, India. The Botanical Survey of India (BSI/SRC/5/23/2024/Tech-235), located in Coimbatore, Tamil Nadu, India, found and verified *A. salviifolium*. Himedia provided us with selenium dioxide ( $\text{SeO}_2$ ). All investigations were carried out using sterile distilled and deionized water.

### 2.2. Preparation of plant extract

The first stage in synthesizing selenium nanoparticles (Se NPs) was the production of the plant extract. Chosen plant materials, including leaves and fruits, were air-dried at ambient temperature for 48h to remove moisture while maintaining their phytochemical integrity. 10g of dried plant material were mixed with 100 mL of distilled water and heated for 30min to facilitate the extraction of bioactive compounds into the solvent. Subsequent to the boiling process, the solution was allowed to settle and was then subjected to filtration utilizing Whatman filter paper in order to get a clear extract, this would act as the chemical that improves and stabilizes in the process of making it.

### 2.3. Green synthesis of Se NPs

In order to produce Se NPs (see Fig. 1-a, b), 10g of plant material and 200mL of distilled water were combined to produce a leaf and fruit extract. After 45min of heating the combination to  $70^\circ\text{C}$  in a heating mantle, the combination was passed through Whatman filter paper to get a clear liquid. Subsequently, selenious acid was made by measuring selenium dioxide and dissolving it in 20 mL of distilled water to make a 1 mM solution of selenious acid ( $\text{H}_2\text{SeO}_3$ ). To make the mixture, combine 30 mL of plant extract with 20 mL of selenious acid solution, and the pH was calibrated to 7.4 using sodium hydroxide ( $\text{NaOH}$ ). The liquid was thereafter enclosed in a conical flask with paper and aluminium foil to avoid contamination. Magnetic stirring was employed for 24h at an appropriate temperature to ensure thorough mixing and facilitate nanoparticle formation. After the process, the mixture was centrifugation at 8500 RPM for 30min to isolate the produced Se Nanoparticles. The resultant nanoparticle pellets were rinsed with distilled water and then dried in a heated oven until thoroughly dehydrated. The desiccated

Se nanoparticles were further pulverized into an ultrafine powder using a mortar and pestle. Ultrasonication was used to suspend the red Se nanoparticles in PBS (pH 7.4), which was then centrifuged for further examination, including UVVis spectroscopy and further characterization methods. This technology offers a simple and eco-friendly technique for producing selenium nanoparticles via the inherent characteristics of plant extracts.

### 2.4. Characterization techniques

#### 2.4.1. UV spectroscopy

The produced Se NPs were examined by UVVis spectroscopy to evaluate their optical characteristics. The Se nanoparticles were first dispersed in distilled water to form a colloidal solution suitable for examination. The absorbance spectra were acquired using a UVVis spectrophotometer, namely the Shimadzu UV-1900i or varian cary spectrophotometers 100, within a wavelength range of 200 nm to 700 nm. Distilled water served as a blank for the spectrophotometer calibration before measurement, guaranteeing precise absorbance results. The absorbance spectrum was periodically scanned to examine the formation and properties of Se NPs, emphasizing the identification of distinct peaks in the UV range, specifically between 200 nm to 300 nm, to confirm successful synthesis and elucidate their optical behaviour.

#### 2.4.2. Fourier transform infrared spectroscopy

To produce transparent discs for analysis, two milligrams of environmentally friendly Se NPs were mixed with one hundred milligrams of potassium bromide (KBr). Utilizing a Japanese-made Bruker IR Affinity apparatus, the generated samples were subjected to Fourier transform infrared (FT-IR) spectroscopy with a wavelength range of 600 to 4000  $\text{cm}^{-1}$  and a resolution of 1  $\text{cm}^{-1}$ . The FT-IR spectrum was obtained using a PerkinElmer spectrophotometer, facilitating the evaluation of functional groups and interactions pertinent to the sustainable synthesis of Se NPs.

#### 2.4.3. X-ray diffraction

The X-ray diffractometer (Philips PAN analytical) utilizing  $\text{CuK}\alpha$  radiation with a wavelength of  $\lambda = 1.541874 \text{ \AA}$  was used to examine the crystalline structure and purity of the produced Se nanoparticles. Data collection occurred on August 27, 2024, covering a range from  $4.905^\circ$  to  $110.010^\circ$ , with a total of 3528 data points and a step size of  $0.030^\circ$ . The Rietveld refinement did not converge, and no background subtraction or data smoothing was applied. To determine the crystalline size,

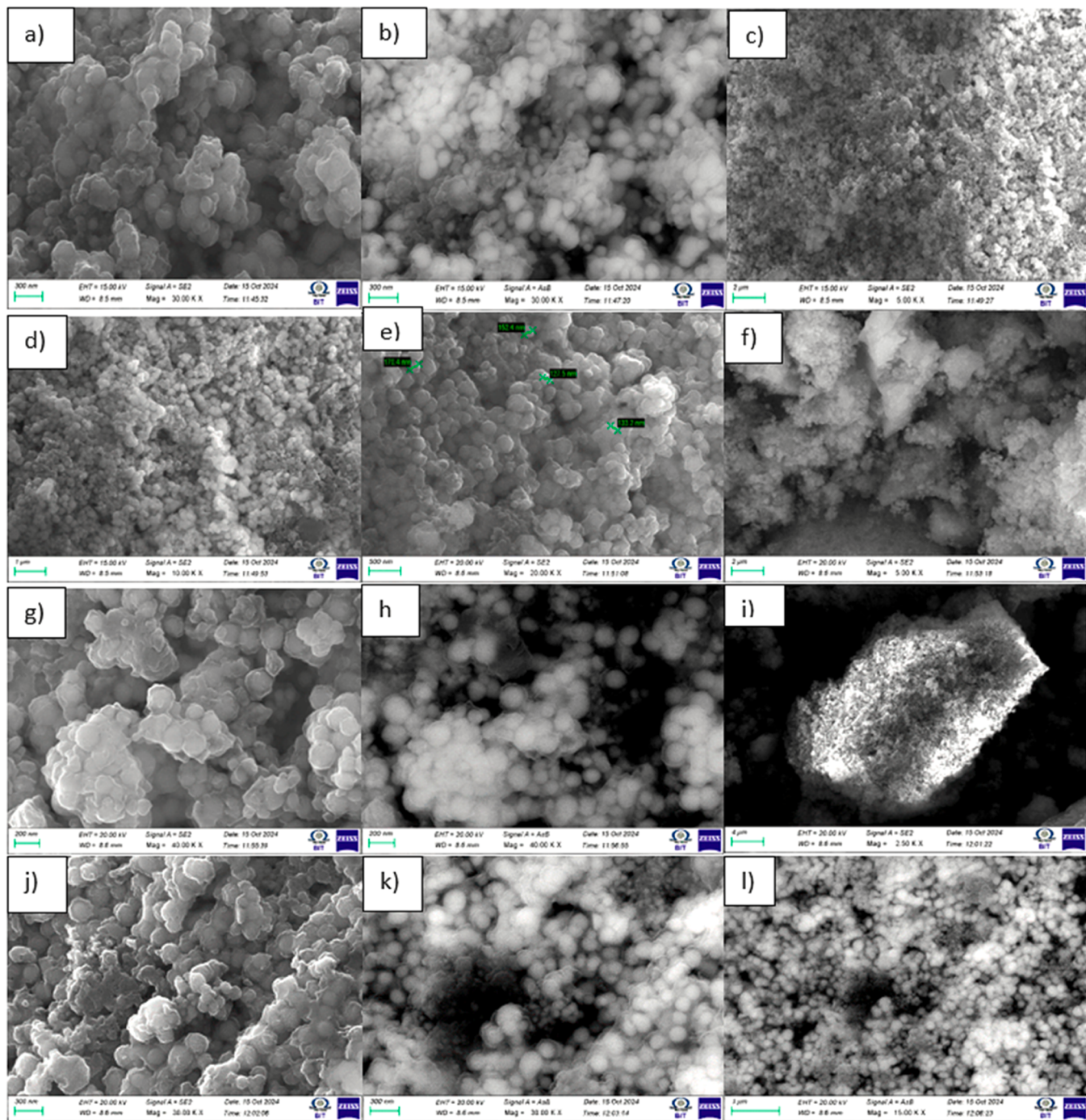


**Fig. 5.** FESEM images of prepared Se NPs in *A. salviifolium* Leaves extract (a) 300 nm SE2 15.00 kV 8.5 mm, (b) 300 nm ASB 15.00 kV 8.5 mm, (c) 2 μm ASB 15.00 kV 8.5 mm, (d) 1 μm SE2 15.00 kV 8.5 mm, (e) 500 nm SE2 20.00 kV 8.6 mm, (f) 2 μm SE2 20.00 kV 8.6 mm, (g) 200 nm SE2 20.00 kV 8.6 mm, (h) 200 nm ASB 20.00 kV 8.6 mm, (i) 4 μm SE2 20.00 kV 8.6 mm, (j) 300 nm SE2 20.00 kV 8.6 mm, (k) 300 nm ASB 20.00 kV 8.6 mm, and (l) 1 μm ASB 20.00 kV 8.6 mm.

Scherrer's equation was used:  $D \approx \beta \cos \theta / 0.9\lambda$ , where D is the crystal size,  $\lambda$  is the wavelength of X-rays,  $\theta$  is the Bragg angle, and  $\beta$  is the FWHM of the peak. This research offers significant insights into the structural properties of the produced Se NPs.

#### 2.4.4. Field emission scanning electron microscopy

The synthesized Se nanoparticles were examined by field emission scanning electron microscopy, and their chemical composition was assessed using energy-dispersive X-ray spectroscopy on a ZEISS EVO-MA 10 microscope from Oberkochen, Germany.

#### 2.4.5. High-resolution transmission electron microscopy

HR-TEM with SAED was applied to analyze the structural characteristics of the produced Se NPs using JEOL JSM 1200EX-II microscope. The specimen preparation involved an *in-situ* focused ion beam (FIB) milling process. Key steps included the milling operations for thinning the specimen, followed by the *in-situ* lift-off procedure using an Omniprobe nanomanipulator. The specimen was subsequently placed in a pre-milled trench inside a copper grid, and final thinning was conducted to attain electron transparency. This approach allows for detailed imaging and analysis at the nanoscale.

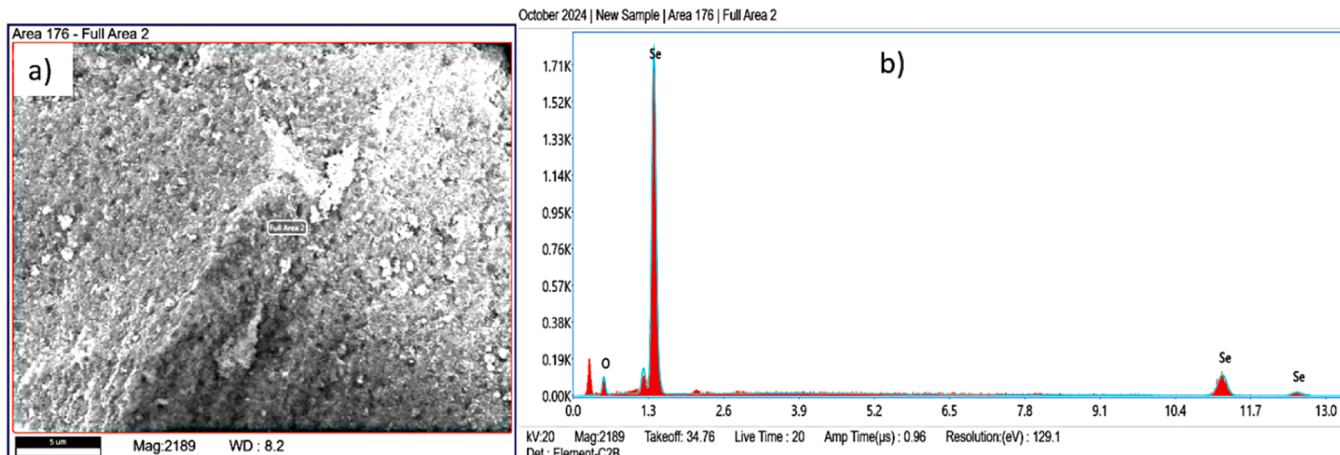


**Fig. 6.** Energy dispersive X-ray spectroscopy in *A. salviifolium* leaves extract a) EDS image of selenium nanoparticles b) EDS spectrum graph of selenium and oxygen.

### 2.5. Antibacterial activity

The antibacterial activity of selenium nanoparticles (Se NPs) synthesized from *A. salviifolium* leaf and fruit extracts was evaluated using the disk diffusion method. Selenium nanoparticles were biosynthesized using extracts from leaves and fruits, utilizing their natural compounds for reduction. A standardized inoculum of the pathogens *Enterococcus faecium* and *Klebsiella pneumoniae* was prepared to ensure consistent results. Mueller-Hinton agar plates were inoculated with the bacterial suspension to create a uniform lawn of growth. Sterile paper disks impregnated with different concentrations of Se NPs (25, 50, and 75 µg/mL) were placed on the agar surface, along with positive controls (Streptomycin) and negative controls (DMSO). The plates were incubated at 37°C for 24h to allow for bacterial growth and interaction with the Se NPs. After incubation, the zones of inhibition around each disk were measured in millimeters to assess the antibacterial effectiveness of the Se NPs against the tested pathogens [13].

## 3. Results and discussion

### 3.1. Plant sources for synthesis of selenium nanoparticles

The plant extract of *A. salviifolium* (Leaves and Fruits) was used in this study (Fig. 1a,b) [14]. Their uncomplicated study shows how to create selenium nanoparticles (Se NPs) using *Artemisia chamaemelifolia* extract in a basic, economical, and environmentally beneficial manner. In the process of creating nanoparticles, this extract works well as a capping and reducing agent. Also, *Moringa oleifera* leaf and bark extracts were used to successfully create synthesized selenium nanoparticles (Se NPs). Bark-derived Se NPs had crystalline peaks and stabilizing functional groups, but leaf-derived Se NPs had a uniform distribution and partial crystallinity [15]. Juices from fresh fruits were extracted by washing, squeezing, and filtering them; they were then centrifuged for 15min at 6000 rpm and kept for later use. After adding 1.44 g/L of selenium solution dropwise to the juices and stirring until the color changed, the mixture was incubated for 48h at room temperature before being centrifuged, cleaned, and dried [16]. After being picked and dried, the *Stellaria media* plant was extracted for 24h using 70 % ethanol in a 1:20 ratio. After that, the extract was lyophilized into powder and concentrated using a rotary evaporator to examine its polyphenol content, antioxidant potential, and antibacterial qualities [17]. In order to make garlic extract, garlic powder was heated in water at 220°C for 25min. It was then filtered and stored at 4°C. To create selenium nanoparticles (Se NPs), the extract was combined with sodium selenite solution, stirred for five hours at 150°C, incubated for four days in the dark, and then centrifuged to produce dry nanoparticles [18]. In the conventional

reaction setup, 20 mL of a 40 mM selenium acid solution was combined with 10 mL of *C. papaya* latex that had been diluted to 50 mL with double-distilled water. The mixture was centrifuged for 10min at 15,000 rpm after being stirred for 24h at room temperature. The pellet that resulted was cleaned, vacuum-dried, and ground into a powder [19].

### 3.2. Synthesis of selenium nanoparticles

Boldo and acerola combos, as well as extracts of onions and acerola, were used to create selenium nanoparticles (Se NPs) at concentrations of 10 and 20 mM using sodium selenite as a precursor. After setting the pH to 7.0, the mixture was incubated for six days at 30°C. This method involved stirring and incubating to encourage the production of nanoparticles, as well as gradually adding acerola extract in a 1:1 ratio [20]. Using sodium selenite as a precursor at different concentrations (0.1 M, 0.01 M, and 0.001 M) combined with plant extracts (1–5 mL) and stirred at 50°C until a color shift was seen, selenium nanoparticles (Se NPs) were created. To finish the synthesis process, the solutions were incubated for a further 24h on an orbital shaker [21]. 0.1 g of sodium selenite was dissolved in 100 mL of double-distilled water to create a stock solution. Then, 1 mL of *Vaccinium arctostaphylos* fruit extract was added to 9 mL of this solution, and the mixture was stirred for 24h until a reddish-brown coloration indicated the creation of Se NP. For additional testing, the resultant nanoparticles were freeze-dried after being purified by centrifugation at 10,000 rpm for ten minutes [22]. By reducing sodium selenite with a methanolic plant extract in a 9:1 ratio and then chilling at 27°C, selenium nanoparticles (Se NPs) were created. A transmission electron microscope (TEM) operating at 80 kV was used to examine the morphology of the biosynthesized Se NPs [23]. In an effort to stabilize the production of Se NP, the experiment employed 0.263 g of sodium selenite in 100 mL of water (10 mM) with Aloevera gel. Aloe Vera gel (0–2 mL), sodium selenite solution (10–20 mL), and *Prunus persica* leaf extract (0–8 mL) were examined in 13 runs using DOE. The samples were then hydrothermally treated for 15min at 121°C and 1.5 bar [24]. As a means to create selenium nanoparticles (Se NPs), heated *Cleistocalyx operculatus* leaf extract was mixed with H<sub>2</sub>SeO<sub>3</sub> solution in different ratios (1:1, 2:1, 3:1, and 4:1) and stirred magnetically for two hours at 40°C. The ensuing dispersion of Se NPs was kept at 5°C [25]. The green biogenesis of selenium nanoparticles (Se-NPs) involved combining 10 mL of OPW extract with 90 mL of 2 mM Na<sub>2</sub>SO<sub>3</sub>, whereas distilled water was used as a reference sample. Three hours of dark incubation on a rotating shaker resulted in the separation, centrifugation, and storage of the Se-NPs at room temperature [26].

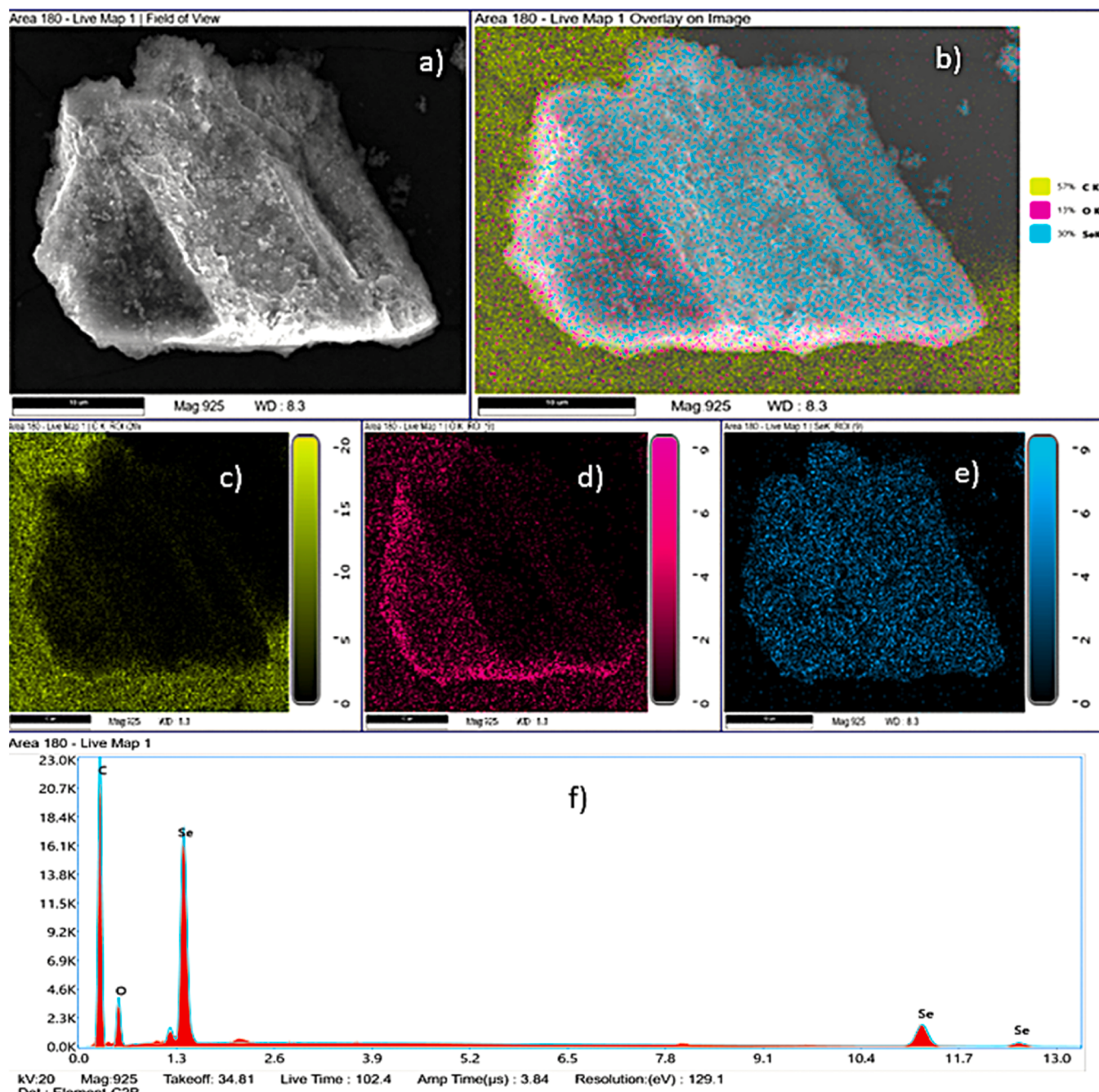


**Fig. 7.** Se NPs elemental mapping in *A. salviifolium* leaf extract a) Live map field of view on leaf Se NPs b) Overlay of Area 180 showing elemental composition (57 % C, 13 % O, 30 % Se) c) Carbon K-edge, indicating the presence of carbon atoms d) Oxygen K-edge, denoting the presence of oxygen atoms e) Selenium K-edge, signifying selenium atoms f) Live map graph of selenium, oxygen and carbon.

### 3.3. UV–Visible spectroscopy

The UVVis spectrophotometric study of Se nanoparticles from samples E10 and E11 demonstrates considerable absorbance ranging from 200 nm to 700 nm, with peak absorbances at 230 nm of 3.927 for E11 and 3.915 for E10. Absorbance decreases with increasing wavelength, reaching values of 0.816 at 300 nm and 0.114 at 700 nm, indicating minimal absorption in the visible range. The similarities in absorbance values suggest good reproducibility, highlighting the potential of Se NPs for applications in photoprotection and UV shielding (Fig. 2a). The UVVis spectrophotometry results for selenium nanoparticles in samples E10 and E11 show strong absorbance peaking at 220 nm, with values of 3.654 for E11 and 3.653 for E10, indicating significant absorption due to

electronic transitions. Absorbance decreases with increasing wavelength, reaching approximately 1.156 at 300 nm and 0.084 at 700 nm, suggesting minimal visible range absorption. The close to proper alignment in absorbance values demonstrates excellent repeatability and consistency, affirming the effective synthesis of selenium nanoparticles (Fig. 2b). UV–Visible spectroscopy measures plasmon resonance and the oscillation of conduction band electrons, confirming nanoparticle (NP) synthesis while providing insights into NP structure, size, aggregation, and stability [27]. Each metallic NP exhibits unique absorbance bands; for example, gold NPs peak between 500 and 550 nm, silver NPs between 400 and 450 nm, and copper NPs from 550 to 600 nm [28]. UV-visible spectroscopy was used to confirm the produced selenium nanoparticles (Se NPs) for the first time. Previous studies further

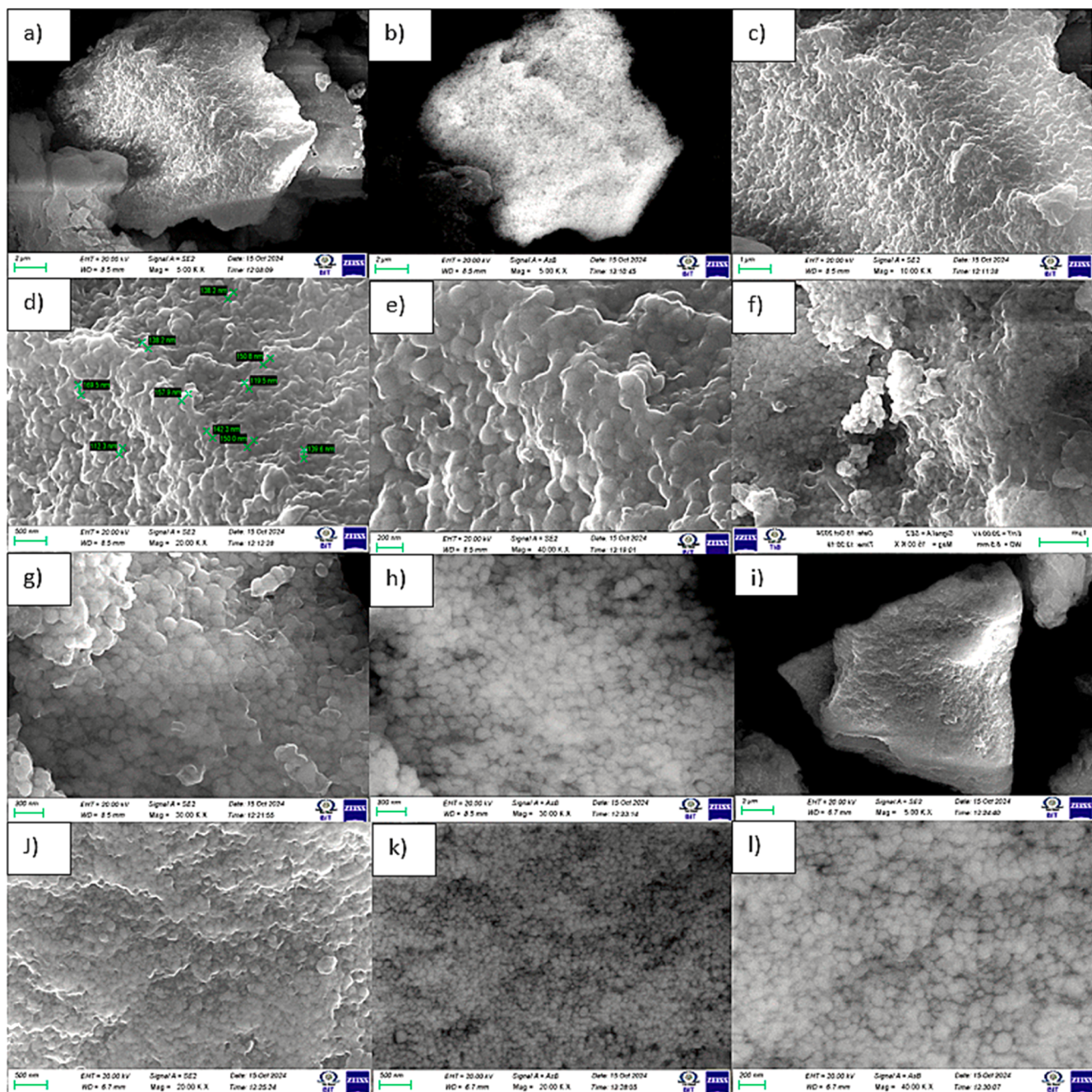


**Fig. 8.** FESEM images of prepared Se NPs in *A. salviifolium* fruits extract (a) 2  $\mu\text{m}$  SE2 20.00 kV 8.5 mm, (b) 2  $\mu\text{m}$  ASB 20.00 kV 8.5 mm, (c) 1  $\mu\text{m}$  SE2 20.00 kV 8.5 mm, (d) 500 nm SE2 20.00 kV 8.5 mm, (e) 200 nm SE2 20.00 kV 8.5 mm, (f) 1  $\mu\text{m}$  SE2 20.00 kV 8.5 mm, (g) 300 nm SE2 20.00 kV 8.5 mm, (h) 300 nm ASB 20.00 kV 8.5 mm, (i) 2  $\mu\text{m}$  SE2 20.00 kV 6.7 mm, (j) 500 nm SE2 20.00 kV 6.7 mm, (k) 500 nm ASB 20.00 kV 6.7 mm, and (l) 200 nm ASB 20.00 kV 6.7 mm.

verified the detection of the maximum absorbance ( $\lambda_{\text{max}}$ ) at 325 nm [29]. A primary peak at 296 nm was detected by UVVis spectroscopy, which is indicative of surface plasmon resonance (SPR) and is connected to the coherent oscillations of freely flowing electrons on the surface of selenium nanoparticles. Furthermore, there were no discernible alterations in the hues for several days following the conclusion of the reaction [30]. Citrus fruit extracts were used to create selenium nanoparticles (Se NPs), which displayed absorbances of roughly 1.5–2 with absorption peaks between 400 and 600 nm. Se nanoparticles (NPs) from grapefruit peels showed maxima at 345 and 550 nm, but those from grapefruit juice showed peaks at 350 and 500 nm [31]. The bio-inspired synthesis of selenium nanoparticles (Se NPs) was investigated using ultraviolet-visible (UVVis) spectroscopy over a wavelength

range of 200 to 800 nm. A peak at 297 nm that was associated with surface plasmon resonance (SPR) was found. Furthermore, there were no discernible changes in the color of the Se NPs for two days following the conclusion of the reaction [32]. Using leaf extract from *Morinda citrifolia*, the creation of selenium nanoparticles (Se NPs) was first confirmed using UV-visible spectroscopy. Measurements were made at six, twelve, twenty-four, forty-eight, and seventy-two hours. In their UV spectrum, the Se NPs showed an absorption peak at 390 nm [33]. UV spectroscopy was used to evaluate the stability of produced selenium nanoparticles (Se NPs), and the results showed a notable peak with maximum absorbance at 350 nm. The findings showed that Se NPs made from tomato plants were quite stable, especially after being incubated for 96h at 37°C [34].

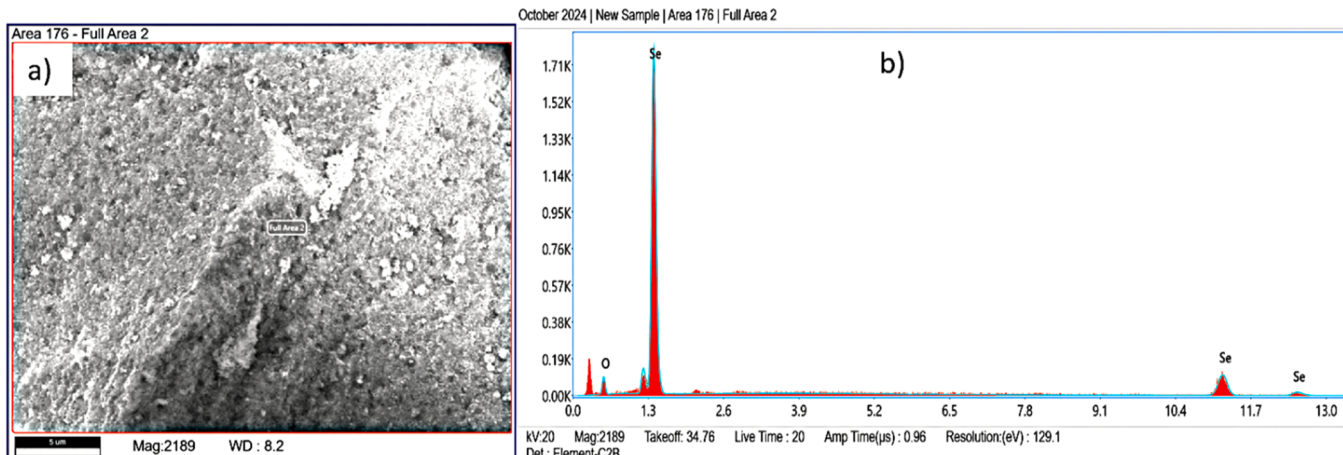


**Fig. 9.** Energy Dispersive X-ray Spectroscopy in *A. salviifolium* fruit extract a) EDS Image of Selenium Nanoparticles b) EDS Spectrum Graph of Selenium and Oxygen.

#### 3.4. Fourier transform infrared spectroscopy

The FT-IR analysis the existence of 6 functional groups responsible for reducing Se ions to biologically active forms and capping biomolecules (Fig. 3a). Peaks at 743.39 cm<sup>-1</sup> (C-H bending, aromatic compounds) and 1258.98 cm<sup>-1</sup> (C-O stretching, alcohols/ethers) indicate the presence of biomolecules acting as reducing and capping agents. Additionally, the 3241.09 cm<sup>-1</sup> peak (O-H stretch, alcohols/phenols) highlights hydroxyl groups role in stabilizing the nanoparticles (Table 1). FT-IR investigation demonstrated interactions between selenium and metabolites from biomass filtrate that may facilitate the synthesis of Se NPs by serving as capping and reducing agents. The spectral analysis of fungal strain As<sup>-1</sup> revealed prominent bands at 1623 cm<sup>-1</sup> corresponding to carbonyl, imine, and alkene functionalities, and at 3291 cm<sup>-1</sup> associated with hydroxyl and amine functionalities. The findings demonstrate that the metabolites are essential for the stabilization and dispersion of the produced Se NPs [35]. The FTIR spectra of selenium nanoparticles had a peak at 1069 cm<sup>-1</sup>, indicating the presence of phenolic groups, whereas the peak at 1252 cm<sup>-1</sup> was associated with polyphenols. The band at 1647 cm<sup>-1</sup> is attributed to O-H stretching vibrations in carboxylic acids. Additionally, peaks around 2936 cm<sup>-1</sup> indicate the existence of lignin, while the band near 3400 cm<sup>-1</sup> denotes N-H bending vibrations [36].

The FT-IR analysis indicated the presence of seven functional groups that reduce Se ions to biologically active forms and cap biomolecules (Fig. 3b). Se NPs fruit extract indicates the involvement of functional groups like O-H stretch (3266.77 cm<sup>-1</sup>) from alcohols/phenols and C=C stretching (1516.63 cm<sup>-1</sup>, 1623.76 cm<sup>-1</sup>) from aromatic compounds in reducing and stabilizing the nanoparticles. Strong peaks like C-H stretching (2917.40 cm<sup>-1</sup>) and C-O stretching (1028.66 cm<sup>-1</sup>) suggest the role of aliphatic compounds and ethers/alcohols in capping the nanoparticles (Table 2). FT-IR analysis of Se NPs showed peaks at 3423 cm<sup>-1</sup> and 1653 cm<sup>-1</sup>, indicating hydroxyl group vibrations, and a peak at 1290 cm<sup>-1</sup> associated with C=O, and -NH<sub>2</sub> functional groups. In addition to functioning as reducing agents when sodium selenite is reduced to elemental selenium, these functional groups also make Se NPs stronger [37]. Four absorption peaks were found in the aqueous extract's FT-IR spectra. At 3410, 2080, 1632 and 1184 cm<sup>-1</sup>, they were situated. The Se NPs spectra peak at 3410 cm<sup>-1</sup>, which showed amino acid N-H and O-H groups, shifted to 3440 cm<sup>-1</sup> [38]. The functional groups in tarragon extract that might stabilize and decrease Se NPs were found using FT-IR spectroscopy. The findings indicated absorption bands linked to several functional groups, including phenols, alcohol, amines and carbonyls. Prominent peaks were seen at about 3390, 1620 and 1430 cm<sup>-1</sup> in the FTIR spectra of the tarragon extract [39].

#### 3.5. X-ray diffractometer

Se NPs showing different peak values demonstrated their crystalline structures, with the most significant peaks being visible (Fig. 4a,b). The XRD pattern of the synthesized Se NPs is presented in results, displaying two distinct regions. A broad shoulder observed between 10° and 30° at low angles indicates the presence of the amorphous phase (a-Se NPs). The XRD patterns of the selected synthesized Se NPs and sodium selenite are shown in result, with distinct strong peaks for sodium selenite at 12, 14.2, 17.5, 19.8, 21.7, 22.3, 24.8, 28, 29.5, 30.8, 34, 36.5, 37.8, 40, 45.8, 50.5, 53.5, 62.5 and 63.8°, indicating a crystalline structure absent in the XRD pattern of SeNPs-1. Comparable results have been recorded by other studies, who noted that the amorphous area is prevalent in synthesized Se NPs [40,41]. By using X-ray powder diffraction (XRD), which showed a clear diffraction pattern suggestive of the trigonal arrangement of L.P.-Se NPs, the structural characteristics of the NPs were examined in more depth. The following Miller indices were represented by the observed peaks: (100), (101), (110), (102), (111), (200), (201), (112), (202), (210), and (113) [42]. The gathered data showed broadening at bragg angle for selenium planes, indicating that the synthesized SC-Se NPs crystal structures matched those in JCPDS file no 659729. Using the Debye-Scherrer equation, the crystal size was calculated to be 32.04 nm based on the bragg angle of the highest peak at 31.68° with an FWHM of 0.450 [43].

#### 3.6. Field emission scanning electron microscopy (FESEM)

The FESEM images indicate a diverse range of selenium nanoparticles (SeNPs) synthesized using leaf extract, with sizes varying from 200 nm to 4 μm. The presence of smaller particles (200 nm to 500 nm) suggests effective synthesis at the nanoscale. Both SE2 and ASB imaging modes reveal consistent particle shapes, predominantly spherical, indicating successful stabilization by the *A. salviifolium* leaf extract. The higher accelerating voltage (20.00 kV) enhances image resolution, allowing for clearer visualization of finer particles. However, the observation of larger particles (up to 4 μm) may suggest agglomeration or incomplete stabilization during synthesis. (Fig. 5.a-l). The spherical shape of SeNPs particle size of glucose is between 100 and 200 nm, whereas other samples exhibit greater agglomeration as a result of surface coating deterioration, stabilizer characteristics, and evaporation. Individual particles, however, are thought to be smaller, at about 100 nm. Both spherical and amorphous SeNPs have been produced using chemical reduction techniques [44]. FESEM analysis revealed SeNPs, a spherical particle ranging from 30 to 200 nm, and MWCNTs, tubular with an inner diameter of 4.5± 0.5 nm and an outer diameter of 10± 1 nm. The composite showed no aggregation or structural distortions,

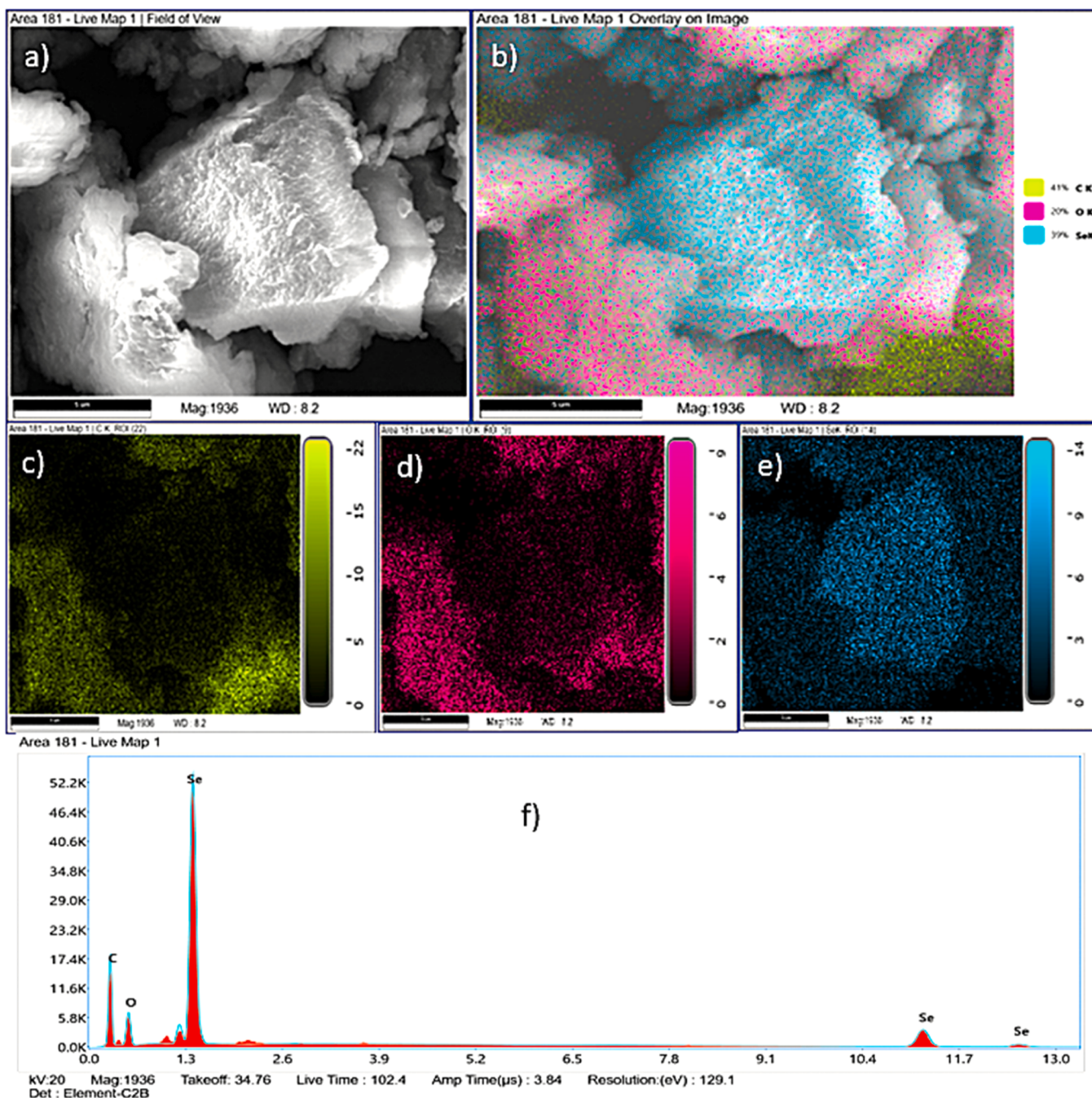


**Fig. 10.** Se NPs Elemental Mapping in *A. salviifolium* fruit extract (a) Live map field of view on leaf Se NPs b) Overlay of Area 180 showing elemental composition (41 % C, 20 % O, 39 % Se) c) Carbon K-edge, indicating the presence of carbon atoms d) Oxygen K-edge, denoting the presence of oxygen atoms e) Selenium K-edge, signifying selenium atoms f) Live map graph of selenium, oxygen and carbon.

confirming nanomaterial stability [45].

The Energy Dispersive X-ray Spectroscopy (EDS) analysis of selenium nanoparticles synthesized using leaf extract was conducted at a magnification of 2189  $\times$ , with a working distance of 182 mm and an accelerating voltage of 20 kV. The takeoff angle was 34.76°, with a live time of 20sec and an amp time of 0.96  $\mu$ s, resulting in a resolution of 129.1. The EDS spectrum identifies selenium (Se) as the predominant element, comprising 91.72 % by weight and 69.17 % by atomic percentage, with a low error percentage of 6.76 %, indicating successful reduction during synthesis. In contrast, oxygen (O) is present at 8.28 % by weight and 30.83 % by atomic percentage, with an error percentage of 16.33 %. The presence of oxygen suggests possible oxidation or interaction with the leaf extract, contributing to nanoparticle stabilization or

functionalization. (Fig. 6.a,b).

The elemental mapping analysis of Area 180 reveals the elemental composition of carbon (C), oxygen (O), and selenium (Se) in the sample, conducted at a magnification of 925  $\times$ , working distance of 8.3 mm, and field of view of 10  $\mu$ m. Carbon is the most abundant element with a weight percentage of 48.63 % and atomic percentage of 77.53 %, followed by selenium at 40.88 % by weight and 9.91 % atomic percentage, and oxygen at 10.49 % by weight and 12.55 % atomic percentage. The net intensities are highest for carbon (907.94), followed by selenium (618.53), and oxygen (376.44). The low error percentage for selenium (3.51 %) confirms its significant presence, while oxygen suggests possible oxidation or interaction during synthesis. The parameters KV:20, takeoff angle:34.81°, live time:102.4sec, amp time:3.84  $\mu$ s, and

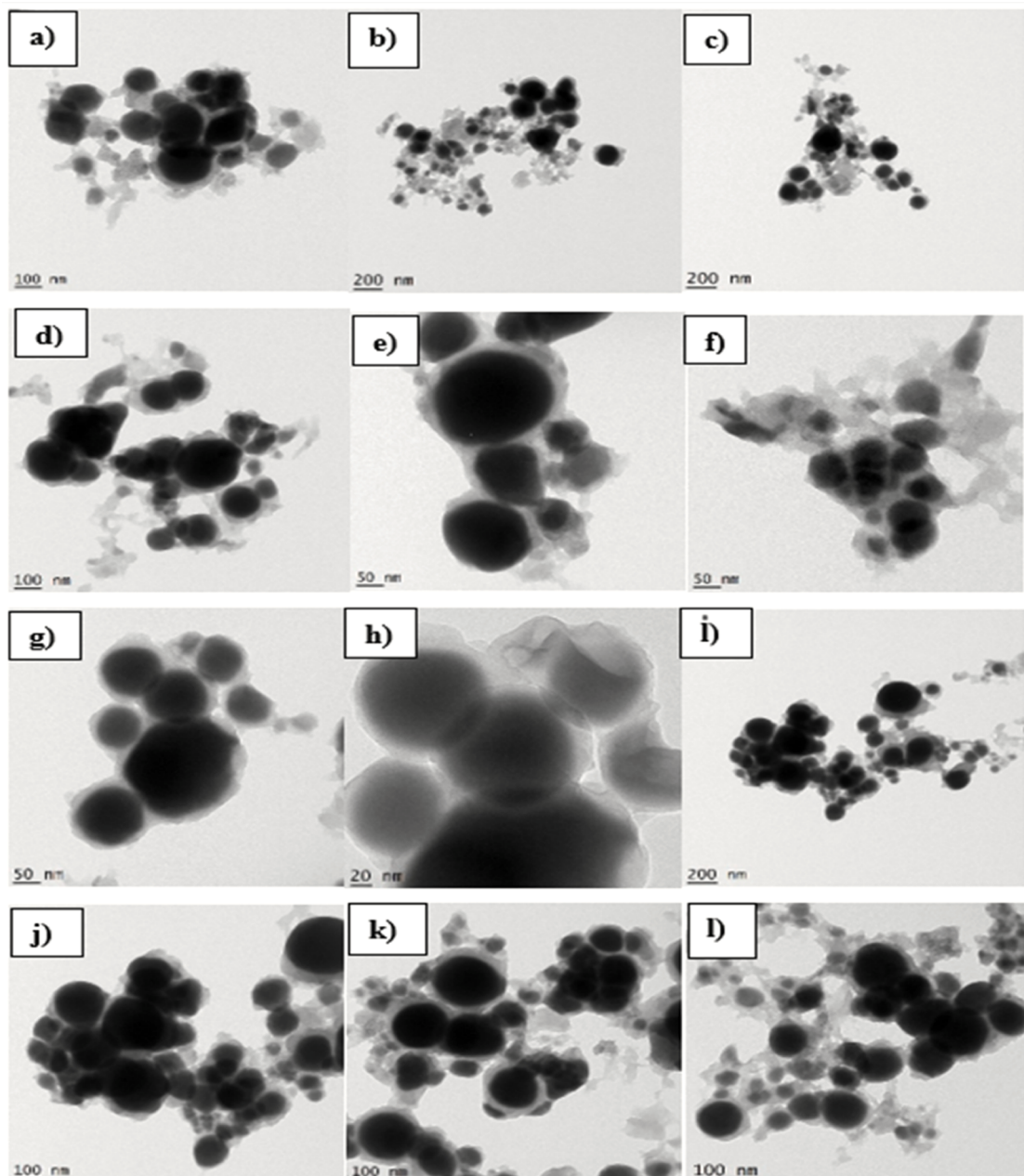


**Fig. 11.** HRTEM images of prepared SeNPs in *A. salviifolium* Leaves extract Se NPs size in a) 100 nm, b) 200 nm, c) 200 nm, d) 100 nm, e) 50 nm, f) 50 nm, g) 50 nm, h) 20 nm, i) 200 nm, j) 100 nm, k) 100 nm, l) 100 nm.

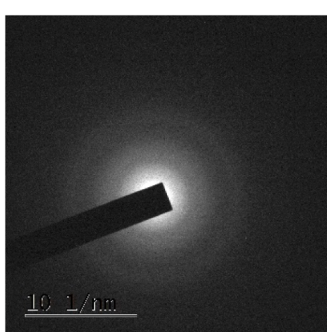


**Fig. 12.** Selected area electron diffraction in Se Nps synthesis *A. salviifolium* Leaves extract.

resolution:129.1 eV ensure precise detection and quantification (Fig.7.a-f). FESEM analysis of the shape of SeNPs showed spherical forms with aggregation zones. A consistent grain size trend was verified by XRD analysis. A prominent peak at 1.5 keV, which corresponds to SeNPs, was found by EDX analysis. The detection of carbon (C) and oxygen (O) signals confirmed the high purity of SeNPs and improved knowledge of their elemental and morphological characteristics [46].

The FESEM analysis of selenium nanoparticles synthesized using fruit extract demonstrates their morphology and size variations across different imaging modes and magnifications. The nanoparticles range from 200 nm to 2  $\mu$ m, with SE2 providing detailed surface topography and ASB highlighting compositional contrast. The consistent use of 20 kV accelerating voltage and varying working distances (8.5 mm and 6.7 mm) ensures precise imaging, confirming uniform synthesis and structural integrity (Fig. 8.a-l). SEM examination revealed the presence of green-synthesised Selenium nanoparticles (Se NPs) on the surface of

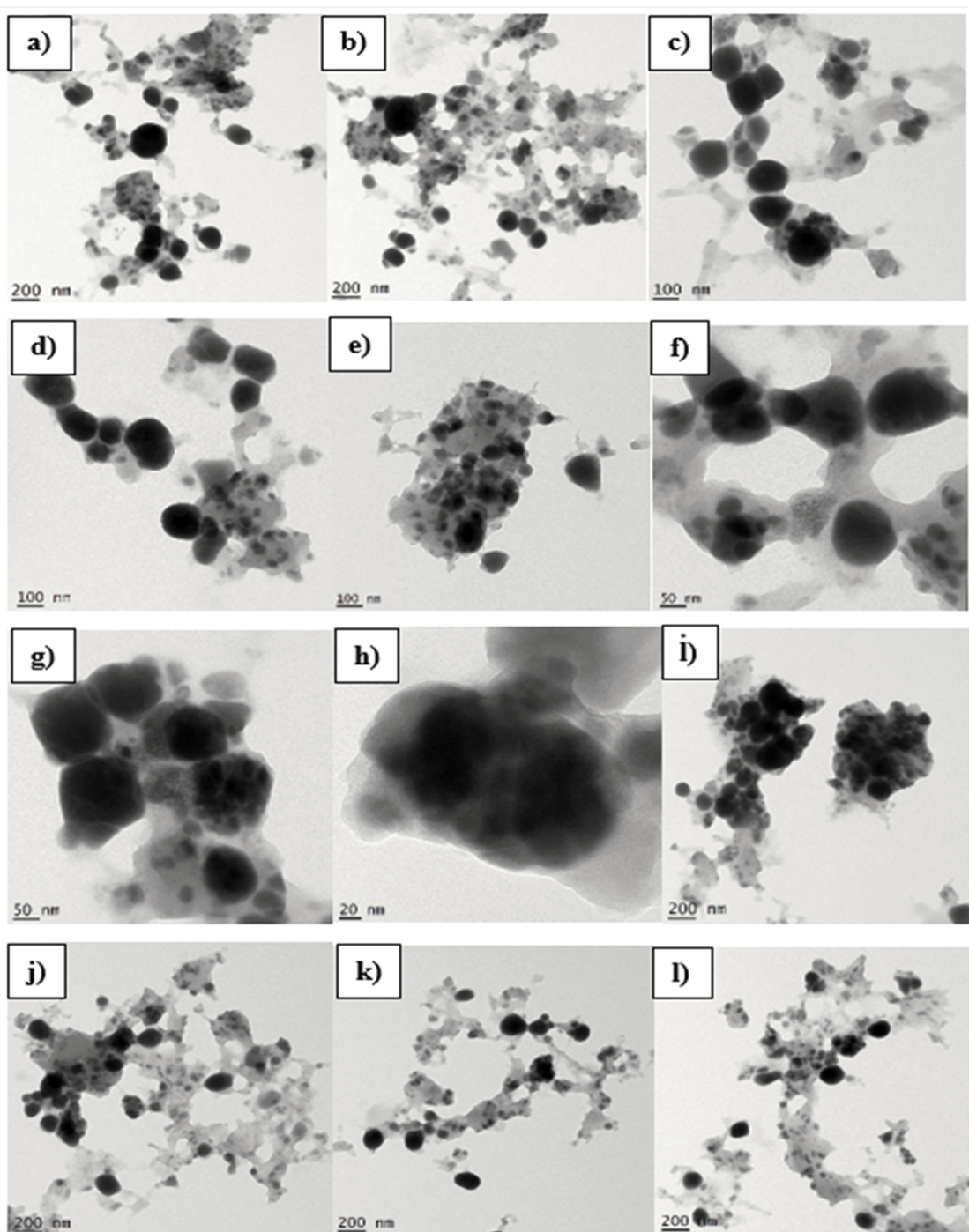


**Fig. 13.** HRTEM images of prepared Se NPs in *A. salviifolium* fruit extract Se NPs particle size a) 200 nm, b) 200 nm, c) 100 nm, d) 100 nm, e) 100 nm, f) 50 nm, g) 50 nm, h) 20 nm, i) 200 nm, j) 200 nm, k) 200 nm, l) 200 nm.

bacterial biomass treated with sodium selenite (2 mM). The nanoparticles, with an average size of  $45.06 \pm 20.02$  nm, were detachable after alkaline lysis, demonstrating the successful synthesis and structural characterisation of Se NPs [47].

The Energy Dispersive X-ray Spectroscopy (EDS) analysis of green-synthesized selenium nanoparticles using fruit extract reveals the elemental composition. Selenium (Se) is the dominant element, constituting 92.67 % by weight and 71.93 % by atomic percentage, indicating successful reduction and stabilization of selenium nanoparticles. Oxygen (O) is present at 7.33 % by weight and 28.07 % by atomic percentage, likely due to surface oxidation or the presence of organic capping agents

from the fruit extract, which aid in nanoparticle stabilization and prevent aggregation (Fig. 9.a,b). FESEM microscopy results show spherical Se particles, ranging from 41 to 44 nm, created using the first method, with their electrical and optical characteristics significantly influenced by their form [48].

The EDS analysis confirms the successful green synthesis of selenium nanoparticles (Se NPs) using fruit extract. Carbon (48.63 % by weight, 77.53 % atomic) is the dominant element, indicating the presence of organic compounds from the fruit extract, which act as stabilizing agents. Oxygen (10.49 % by weight, 12.55 % atomic) is likely due to surface oxidation or functional groups in the organic matrix,

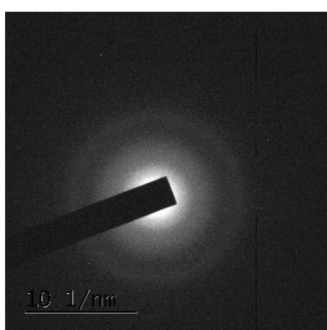


**Fig. 14.** Selected Area Electron Diffraction in Se Nps synthesis *A.salviifolium* fruit extract.

**Table 3**  
Details of antibacterial activity of *A.salviifolium* leaf synthesize SeNPs.

S. No	Name of the pathogens	Zone of inhibition (mm) SeNPs in leaf extract of <i>A. salviifolium</i>				
		Positive Control (Streptomycin)	Negative Control (DMSO)	Concentration ( $\mu\text{g/mL}$ )		
		25	50	75		
1	<i>Enterococcus faecium</i>	20 $\pm$ 0.26 mm		7	13	11
				$\pm$ 0.21	$\pm$ 0.15	$\pm$ 0.60
2	<i>Klebsiella pneumoniae</i>	21 $\pm$ 0.63 mm		9	16	12
				$\pm$ 0.33	$\pm$ 0.24	$\pm$ 0.24

**Table 4**  
Details of antibacterial activity of *A.salviifolium* fruit synthesize SeNPs.

S. No	Name of the pathogens	Zone of inhibition (mm) SeNPs in fruit extract of <i>A. salviifolium</i>				
		Positive Control (Streptomycin)	Negative Control (DMSO)	Concentration ( $\mu\text{g/mL}$ )		
		25	50	75		
1	<i>Enterococcus faecium</i>	22 $\pm$ 0.28 mm		6	9	7
				$\pm$ 0.21	$\pm$ 0.20	$\pm$ 0.19
2	<i>Klebsiella pneumoniae</i>	19 $\pm$ 0.26 mm		8	10	6
				$\pm$ 0.23	$\pm$ 0.31	$\pm$ 0.15

contributing to nanoparticle stability. Selenium (40.88 % by weight, 9.91 % atomic) confirms the formation of Se NPs, with its lower atomic percentage reflecting the organic material's dominance. The organic matrix plays a key role in stabilizing and functionalizing the nanoparticles (Fig. 10.a-f). The spectral peak of selenium, a selenium element, was found to be the source of the carbon (C) and oxygen (O) elements. However, due to weak signals, two peaks between 112 eV and 12.5 eV nearly vanished, indicating the presence of SeNPs [49].

### 3.7. High-Resolution transmission electron microscopy (HR-TEM)

The HRTEM analysis of green-synthesized Selenium nanoparticles (Se NPs) using *A.salviifolium* leaf extract reveals a wide range of particle sizes, from 20 nm to 200 nm. The nanoparticles are categorized into three distinct size groups: larger particles (200 nm), medium-sized particles (100 nm), and smaller particles (50 nm), with the smallest observed particle being 20 nm. This diversity highlights the effectiveness of the green synthesis method in producing Se NPs with tailored dimensions. Smaller nanoparticles (20–50 nm) are particularly notable for their enhanced biological activity due to their high surface-area-to-volume ratio. (Fig. 11.a-l).

The SAED pattern confirms the crystalline nature of selenium nanoparticles, revealing ordered atomic planes with 0.1 nm spacing. Miller indices are identified through discrete spots and sharp rings, demonstrating leaf extract's effective stabilizing and lowering

properties (Fig. 12).

The High-Resolution Transmission Electron Microscopy (HRTEM) analysis of green-synthesized Selenium nanoparticles (Se NPs) using *A. salviifolium* fruit extract reveals a size distribution ranging from 20 nm to 200 nm. The majority of the particles are larger, measuring 200 nm, which indicates a preference for larger nanoparticle formation during synthesis. Medium-sized particles measuring 100 nm are also observed, showing consistency in this size range. Smaller particles measuring 50 nm are present in fewer instances, and the smallest particle measures 20 nm. This characterization highlights the successful synthesis of Se NPs with varied sizes, demonstrating the effectiveness of fruit extract in producing nanoparticles with tailored dimensions. (Fig. 13).

The HR-TEM pictures indicate that a droplet of the sample was deposited on copper grids and let to evaporate gradually at ambient temperature. The resultant picture clearly demonstrates that the Se NPs produced from cow urine are spherical, display little aggregation, and are uniformly disseminated [50]. In accordance with XRD results, the average particle size of selenium nanoparticles produced using a green technique is 11 nm, according to TEM/HRTEM and SAED investigations. The HR-TEM pictures show a distinct inner surface, with d-width of 0.282 nm, which match to the nanoparticles' (101) plane [51]. Purified selenium nanoparticles (Se-NPs) have a spherical form, size, and an organic shell layer, as seen by their transmission electron micrograph. The particle dimensions are in agreement with the DLS findings. Furthermore, TEM-EDX examination verifies the existence of selenium in addition to carbon, oxygen, and copper, demonstrating the stability and amorphous nature of the nanoparticles [52].

The SAED pattern confirms the crystalline nature of selenium nanoparticles, revealing well-ordered atomic groupings with a 10 1/nm spacing. Fruit extract successfully promoted the synthesis of ordered structures, improving electrical, optical, and catalytic qualities, making them useful for various activities (Fig. 14).

### 3.8. Antibacterial activity of *A.salviifolium* extracts in SeNPs

(*A.salviifolium* leaf extract synthesized SeNPs): *Enterococcus faecium* showed a zone of inhibition of 20 $\pm$  0.26 mm at a concentration of 25  $\mu\text{g}/\text{mL}$ , which increased to 13 $\pm$  0.15 mm at 50  $\mu\text{g}/\text{mL}$  and decreased to 11 $\pm$  0.60 mm at 75  $\mu\text{g}/\text{mL}$ . *Klebsiella pneumoniae* exhibited a higher zone of inhibition at 21 $\pm$  0.63 mm for the same concentration, with values of 16  $\pm$  0.24 mm at 50  $\mu\text{g}/\text{mL}$  and 12 $\pm$  0.24 mm at 75  $\mu\text{g}/\text{mL}$  (Table 3) [53]. elucidate how selenium nanoparticles (Se NPs), particularly the smaller spherical ones (50–100 nm), have antibacterial activity against both Gram-positive and Gram-negative bacteria and can infiltrate bacterial cells with ease. Gram-positive bacteria have a stronger peptidoglycan layer that affects their sensitivity, but Gram-negative bacteria are more vulnerable because of their negatively charged lipopolysaccharide coating.

(*A. salviifolium* fruit extract synthesized Se NPs): For *Enterococcus faecium*, the zone of inhibition was slightly higher at 22 $\pm$  0.28 mm at 25  $\mu\text{g}/\text{mL}$  but decreased to lower values with increased concentrations. *Klebsiella pneumoniae* showed a reduced effect compared to leaf extracts, with zones of inhibition of 19 $\pm$  0.26 mm at 25  $\mu\text{g}/\text{mL}$ , decreasing further with higher concentrations (Table 4) [13]. outlined how oxidative damage, mechanical disruption to cell membranes, and the release of Se ions—whose increased surface area enhances interaction—are the antibacterial actions of selenium nanoparticles (Se NPs) against *S. aureus*. The increased surface area and adsorption capability of APT increase bacterial interaction, which enhances the antibacterial properties of the Se/APT nanocomposite. Antibiotic cefotaxime, despite its effectiveness against various bacterial strains, has a minimum inhibitory concentration (MIC) that is significantly lower than SeNPs, particularly against MDR [54].

#### 4. Conclusions

In conclusion, our study effectively demonstrated the green synthesis of Se NPs using natural extracts from *A. salviifolium* leaves and fruits, successfully demonstrates the green synthesis of selenium nanoparticles (Se NPs) using plant extracts or biological agents, which act as reducing and stabilizing agents. This eco-friendly and cost-effective approach eliminates the need for toxic stabilizers, ensuring high stability and biocompatibility of the nanoparticles. The characterization techniques employed confirm the successful synthesis and properties of Se NPs, UVVis Spectroscopy exhibits characteristic absorption peaks, confirming nanoparticle formation. FTIR analysis identifies functional groups responsible for reduction and stabilization. XRD confirms the crystalline nature of selenium nanoparticles through specific diffraction patterns. FESEM with EDS reveals uniform morphology, size distribution, and elemental composition of the nanoparticles. HRTEM with SAED provides detailed nanoscale imaging, confirming spherical shape, uniform size, and crystallinity. The antibacterial activity of *A. salviifolium*-Se NPs demonstrate that selenium nanoparticles (Se NPs) synthesized from both leaf and fruit extracts possess antibacterial activity against the tested pathogens, with varying effectiveness based on concentration and extract type. Leaf extracts generally produced higher zones of inhibition than fruit extracts, indicating that leaf phytochemicals may enhance the antibacterial properties of Se NPs. This study underscores the potential of utilizing plant extracts for the green synthesis of nanoparticles in biomedical applications to combat bacterial infections.

#### CRediT authorship contribution statement

**Karunya Saravanan:** Writing – review & editing, Writing – original draft, Visualization, Validation, Supervision, Project administration, Methodology, Investigation. **Manivannan Madhaiyan:** Visualization, Investigation, Formal analysis. **Prabu Periyasamy:** Validation, Investigation, Formal analysis. **Prasath Manivannan:** Investigation, Funding acquisition, Formal analysis, Conceptualization. **Alpaslan Bayrakdar:** Funding acquisition, Formal analysis. **V. Balakrishnan:** Writing – review & editing, Supervision, Funding acquisition, Data curation, Conceptualization.

#### Declaration of competing interest

The authors declare that they have no known competing financial interests or personal relationships that could have appeared to influence the work reported in this research article.

#### Acknowledgments

The authors recognize and thank the Department of Botany, School of Life sciences, Periyar University, Salem, Tamil Nadu, India, for providing infrastructural facility. The authors are thankful the Directorate of Collegiate Education, Chennai (Ref.R.C.No.00160/L/2022 dated 11.12.2023) (Under the Higher Education Department, Government of Tamil Nadu, India).

#### Data availability

The data that has been used is confidential.

#### References

- [1] M.A. Khudier, H.A. Hammadi, H.T. Atyia, H. Al-Karagoly, S. Albukhaty, G. M. Sulaiman, Y.H. Dewir, H.B. Mahood, Antibacterial activity of green synthesized selenium nanoparticles using *Vaccinium arctostaphylos* (L.) fruit extract, Cogent Food Agric. 9 (2023) 2245612, <https://doi.org/10.1080/23311932.2023.2245612>.
- [2] A. Husen, K.S. Siddiqi, Plants and microbes assisted selenium nanoparticles: characterization and application, Sustain. Chem. Pharm. 1 (2014) 28–41, <https://doi.org/10.1186/s12951-014-0028-6>.
- [3] S. Nag, S. Kar, S. Mishra, B. Stany, A. Seelan, S. Mohanto, C. Kamaraj, V. Subramaniyan, Unveiling green synthesis and biomedical theranostic paradigms of selenium nanoparticles (Se NPs)—A state-of-the-art comprehensive update, Int. J. Pharm. 659 (2024) 124535, <https://doi.org/10.1016/j.ijpharm.2024.124535>.
- [4] W. Lu, Z. Li, M. Feng, L. Zheng, S. Liu, B. Yan, J.S. Hu, D.J. Xue, Structure of amorphous selenium: small ring, big controversy, J. Am. Chem. Soc. 146 (2024) 6345–6351, <https://doi.org/10.1021/jacs.4c00219>.
- [5] S. Jubie, N. Jawahar, R. Koshy, B. Gowramma, V. Murugan, B. Suresh, Anti-arthritis activity of bark extracts of *Alangium salviifolium* Wang, Rasayan J. Chem. 1 (2008) 433–436.
- [6] R.P. Mondal, A. Ghosh, S. Burman, G. Chandra, Efficacy of ethyl acetate extract of *Alangium salviifolium* fruit pericarp against *Culex quinquefasciatus* larvae, Notulae Scientia Biologicae 14 (2022) 11251, <https://doi.org/10.55779/nsb14211251>.
- [7] I.A. Ali, A.B. Ahmed, H.I. Al-Ahmed, Green synthesis and characterization of silver nanoparticles for reducing the damage to sperm parameters in diabetic compared to metformin, Sci. Rep. 13 (2023) 2256, <https://doi.org/10.1038/s41598-023-29412-3>.
- [8] I.A. Mohammed Ali, H.I. AL-Ahmed, A.B. Ahmed, Evaluation of green synthesis (*Withania somnifera*) of selenium nanoparticles to reduce sperm DNA fragmentation diabetic mice induced with streptozotocin, Appl. Sci. 13 (2023) 728, <https://doi.org/10.3390/app13020728>.
- [9] X. Qin, Z. Wang, J. Lai, Y. Liang, K. Qian, The Synthesis of Selenium Nanoparticles and Their Applications in Enhancing Plant Stress Resistance: a Review, Nanomaterials 15 (2025) 301, <https://doi.org/10.3390/nano15040301>.
- [10] D. Kirubakaran, J.B. Wahid, N. Karmegam, R. Jeevika, L. Sellappillai, M. Rajkumar, K.J. SenthilKumar, A comprehensive review on the green synthesis of nanoparticles: advancements in biomedical and environmental applications, Biomed. Mater. Dev. (2025) 1–26, <https://doi.org/10.1007/s41474-025-00295-4>.
- [11] N. Roy, T. Nivedya, P. Paira, R. Chakrabarty, Selenium-based nanomaterials: green and conventional synthesis methods, applications, and advances in dye degradation, RSC. Adv. 15 (2025) 3008–3025, <https://doi.org/10.3390/dietetics4010006>.
- [12] M. Ikram, B. Javed, N.I. Raja, Z.U. Mashwani, Biomedical potential of plant-based selenium nanoparticles: a comprehensive review on therapeutic and mechanistic aspects, Int. J. Nanomedicine (2021) 249–268, <https://doi.org/10.2147/IJN.S295053>. Jan 12.
- [13] N.S. Shehata, B.H. Elwakil, S.S. Elshewemi, D.A. Ghareeb, Z.A. Olama, Selenium nanoparticles coated bacterial polysaccharide with potent antimicrobial and anti-lung cancer activities, Sci. Rep. 13 (2023) 21871, <https://doi.org/10.1038/s41598-023-48921-9>.
- [14] Z. Keshtmand, E. Khademian, P.P. Jafroodi, M.S. Abtahi, M.T. Yaraki, Green synthesis of selenium nanoparticles using *Artemisia chamaemelifolia*: toxicity effects through regulation of gene expression for cancer cells and bacteria, Nano-Struct. Nano-Objects 36 (2023) 101049, <https://doi.org/10.1016/j.nanoso.2023.101049>.
- [15] A.B. Olaoye, S.S. Owoeye, J.S. Nwobegu, Facile green synthesis of plant-mediated selenium nanoparticles (SeNPs) using *Moringa oleifera* leaf and bark extract for targeting  $\alpha$ -amylase and  $\alpha$ -glucosidase enzymes in diabetes management, Hybrid Adv. 7 (2024) 100281, <https://doi.org/10.1016/j.hybadv.2024.100281>.
- [16] R. Shirmehendi, S. Javanshir, M. Honarmand, A green approach to the bio-based synthesis of selenium nanoparticles from mining waste, J. Clust. Sci. 32 (2021) 1311–1323, <https://doi.org/10.1007/s10876-020-01892-7>.
- [17] F.G. Miere, M. Gamea, A.G. Teodorescu, L. Fritea, M. Lestyan, T. Horvath, A. Hanga-Fărcaş, S.I. Vicaş, The green synthesis of silver and selenium nanoparticles using the plant *Stellaria media* (L.) Vill, Pharmacophore 13 (2022) 88–95, <https://doi.org/10.51847/rzjBEulH9c>.
- [18] Z. Younas Ahmad, Z.U. Mashwani, N.I. Raja, A. Akram, Phytomediated selenium nanoparticles improved physio-morphological, antioxidant, and oil bioactive compounds of sesame under induced biotic stress, ACS. Omega 8 (2023) 3354–3366, <https://doi.org/10.1021/acsomega.2c07084>.
- [19] S. Rajasekar, S. Kuppusamy, Eco-friendly formulation of selenium nanoparticles and its functional characterization against breast cancer and normal cells, J. Clust. Sci. 32 (2021) 907–915, <https://doi.org/10.1007/s10876-020-01856-x>.
- [20] L.M. dos Santos Souza, M. Dibo, J.J. Sarmiento, A.B. Seabra, L.P. Medeiros, I. M. Lourenço, R.K. Kobayashi, G. Nakazato, Biosynthesis of selenium nanoparticles using combinations of plant extracts and their antibacterial activity, Curr. Res. Green Sustain. Chem. 5 (2022) 100303, <https://doi.org/10.1016/j.crgsc.2022.100303>.
- [21] J.P. Dash, L. Mani, S.K. Nayak, Antibacterial activity of *Blumea axillaris*-synthesized selenium nanoparticles against multidrug-resistant pathogens of aquatic origin, Egypt. J. Basic Appl. Sci. 9 (2022) 65–76, <https://doi.org/10.1080/2314808X.2021.2019949>.
- [22] M.A. Khudier, H.A. Hammadi, H.T. Atyia, H. Al-Karagoly, S. Albukhaty, G. M. Sulaiman, Y.H. Dewir, H.B. Mahood, Antibacterial activity of green synthesized selenium nanoparticles using *Vaccinium arctostaphylos* (L.) fruit extract, Cogent Food Agric. 9 (2023) 2245612, <https://doi.org/10.1080/23311932.2023.2245612>.
- [23] M.A. Hawsah, R. Abdel-Gaber, S. Al-Quraishy, H.M. Aljawdah, S.N. Maoodaa, E. Al-Shaeby, Green synthesis of selenium nanoparticles using *Azadirachta indica* leaves extract: evaluation of antihelmintic and biocompatibility potential, Food Sci. Technol. 43 (2023), <https://doi.org/10.5327/fst.13223>.
- [24] S. Shayan, D. Hajihajkolai, F. Ghazale, F. Gharahdaghigharahtappeh, A. Faghih, O. Ahmadi, G. Behbudi, Optimization of green synthesis formulation of selenium nanoparticles (Se NPs) using peach tree leaf extract and investigating its properties

- and stability, *Iran. J. Biotechnol.* 22 (2024) e3786, <https://doi.org/10.30498/ijb.2024.413943.3786>.
- [25] T.T. Vu, P.T. Nguyen, N.H. Pham, T.H. Le, T.H. Nguyen, D.T. Do, D.D. La, Green synthesis of selenium nanoparticles using *Cleistocalyx operculatus* leaf extract and their acute oral toxicity study, *J. Compos. Sci.* 6 (2022) 307, <https://doi.org/10.3390/jcs6100307>.
- [26] S.S. Salem, M.S. Badawy, A.A. Al-Askar, A.A. Arishi, F.M. Elkady, A.H. Hashem, Green biosynthesis of selenium nanoparticles using orange peel waste: characterization, antibacterial and antibiofilm activities against multidrug-resistant bacteria, *Life* 12 (2022) 893, <https://doi.org/10.3390/life12060893>.
- [27] M. Shahbaz, A. Akram, N.I. Raja, T. Mukhtar, Z.U. Mashwani, A. Mehmak, N. Fatima, S. Sarwar, E.U. Haq, T. Yousaf, Green synthesis and characterization of selenium nanoparticles and its application in plant disease management: a review, *Pakistan J. Phytopathol.* 34 (2022) 189–202, <https://doi.org/10.33866/phytopathol.034.01.0739>.
- [28] S.Patil Puri, *Tinospora cordifolia* stem extract-mediated green synthesis of selenium nanoparticles and its biological applications, *Pharmacognosy. Res.* 14 (2022), <https://doi.org/10.5530/pj.2019.11.x>.
- [29] S. Perumal, M.V. Gopal Samy, D. Subramanian, Selenium nanoparticle synthesis from endangered medicinal herb (*Ericostoma axillare*), *Bioprocess. Biosyst. Eng.* 44 (2021) 1853–1863, <https://doi.org/10.1007/s00449-021-02565-z>.
- [30] A.S. Alhawiti, Citric acid-mediated green synthesis of selenium nanoparticles: antioxidant, antimicrobial, and anticoagulant potential applications, *BioMass Convers. Biorefin.* 14 (2024) 6581–6590, <https://doi.org/10.1007/s13399-022-02798-2>.
- [31] G.B. Alvi, M.S. Iqbal, M.M. Ghaith, A. Haseeb, B. Ahmed, M.I. Qadir, Biogenic selenium nanoparticles (Se NPs) from citrus fruit have anti-bacterial activities, *Sci. Rep.* 11 (2021) 4811, <https://doi.org/10.1038/s41598-021-84099-8>.
- [32] B.A. Al Jahdaly, N.S. Al-Radadi, G.M. Eldin, A. Almahri, M.K. Ahmed, K. Shoueir, I. Janowska, Selenium nanoparticles synthesized using an eco-friendly method: dye decolorization from aqueous solutions, cell viability, antioxidant, and antibacterial effectiveness, *J. Mater. Res. Technol.* 11 (2021) 85–97, <https://doi.org/10.1016/j.jmrt.2020.12.098>.
- [33] M. Nagalingam, S. Rajeshkumar, S.K. Balu, M. Tharani, K. Arunachalam, Anticancer and antioxidant activity of *Morinda citrifolia* leaf-mediated selenium nanoparticles, 2022 (2022) 2155772, <https://doi.org/10.1155/2022/2155772>.
- [34] M.S. Iqbal, K. Abbas, M.I. Qadir, Synthesis, characterization and evaluation of biological properties of selenium nanoparticles from *Solanum lycopersicum*, *Arab. J. Chem.* 15 (2022) 103901, <https://doi.org/10.1016/j.arabjc.2022.103901>.
- [35] S.S. Salem, M.M. Fouda, A. Fouda, M.A. Awad, E.M. Al-Olayan, A.A. Allam, T. I. Shaheen, Antibacterial, cytotoxicity and larvicidal activity of green synthesized selenium nanoparticles using *Penicillium corylophilum*, *J. Clust. Sci.* 32 (2021) 351–361, <https://doi.org/10.1007/s10876-020-01794-8>.
- [36] R.S. Ghaderi, F. Adibian, Z. Sabouri, J. Davoodi, M. Kazemi, S.A. Jamehdar, Z. Meshkat, S. Soleimanpour, M. Daroudi, Green synthesis of selenium nanoparticles by *Abelmoschus esculentus* extract and assessment of its antibacterial activity, *Mater. Technol.* 37 (2022) 1289–1297, <https://doi.org/10.1080/10667857.2021.1935602>.
- [37] M. Safaei, H.R. Mozaffari, H. Moradpoor, M.M. Imani, R. Sharifi, A. Golshah, Optimization of green synthesis of selenium nanoparticles and evaluation of their antifungal activity against oral *Candida albicans* infection, *Adv. Mater. Sci. Eng.* 2022 (2022) 1376998, <https://doi.org/10.1155/2022/1376998>.
- [38] A. Fouda, W.A. Al-Otaibi, T. Saber, S.M. AlMotwaa, K.S. Alshallash, M. Elhady, N. F. Badr, M.A. Abdel-Rahman, Antimicrobial, antiviral, and in-vitro cytotoxicity and mosquitoicidal activities of *Protulaca oleracea*-based green synthesis of selenium nanoparticles, *J. Funct. Biomater.* 13 (2022) 157, <https://doi.org/10.3390/jfb13030157>.
- [39] M.T. Yilmaz, H. Ispirli, O. Taylan, E. Dertli, A green nano-biosynthesis of selenium nanoparticles with Tarragon extract: structural, thermal, and antimicrobial characterization, *LWT* 141 (2021) 110969, <https://doi.org/10.1016/j.lwt.2021.110969>.
- [40] C. Mellinas, A. Jiménez, M.D. Garrigós, Microwave-assisted green synthesis and antioxidant activity of selenium nanoparticles using *Theobroma cacao* L. bean shell extract, *Molecules* 24 (2019) 4048, <https://doi.org/10.3390/molecules24224048>.
- [41] S. Alipour, S. Kalari, M.H. Morowvat, Z. Sabahi, A. Dehshahri, Green synthesis of selenium nanoparticles by cyanobacterium *Spirulina platensis* (abdf2224): cultivation condition quality controls, *Biomed. Res. Int.* 2021 (2021) 6635297, <https://doi.org/10.1155/2021/6635297>.
- [42] M.M. Desouky, R.H. Abou-Saleh, T.A. Moussa, H.M. Fahmy, Nano-chitosan-coated, green-synthesized selenium nanoparticles as a novel antifungal agent against *Sclerotinia sclerotiorum*: in vitro study, *Sci. Rep.* 15 (2025) 1004, <https://doi.org/10.1038/s41598-024-79574-x>.
- [43] S. Kanber, M. Yildiztekin, M.F. Baran, Eco-friendly synthesis of selenium nanoparticles via *Sternbergia candida*: enhancing antioxidant defense and mitigating salt stress in pepper (*Capiscum annuum* L.) plants, *Chem. Open* (2025), <https://doi.org/10.1002/open.202400341>.
- [44] N. Filipović, D. Ušjak, M.T. Milenković, K. Zheng, L. Liverani, A.R. Boccaccini, M. M. Stevanović, Comparative study of the antimicrobial activity of selenium nanoparticles with different surface chemistry and structure, *Front. Bioeng. Biotechnol.* 8 (2021) 624621, <https://doi.org/10.3389/fbioe.2020.624621>.
- [45] T. Garg, A. Joshi, A. Kumar, V. Kumar, N. Jindal, A. Awasthi, S. Kaur, Foliar application of selenium nanoparticles, multiwalled carbon nanotubes and their hybrids stimulates plant growth and yield characters in rice (*Oryza sativa* L.) under salt stress, *Plant Nano Biol.* (2025) 100146, <https://doi.org/10.1016/j.planta.2025.100146>.
- [46] N.F. Shehab, N.H. Hasan, H.K. Ismail, Investigating the Alkaline Potential of Mineral Trioxide Aggregate Repair Using Selenium Nanoparticles, *Braz. Dent. J.* 35 (2024) e24–5760, <https://doi.org/10.1590/0103-6440202405760>.
- [47] M. Ashengroh, S.R. Hosseini, A newly isolated *Bacillus amylobiotaceus* SRB04 for the synthesis of selenium nanoparticles with potential antibacterial properties, *Int. Microbiol.* 24 (2021) 103–114, <https://doi.org/10.1007/s10123-020-00147-9>.
- [48] B.K. Buraa, B.H. Adil, A.Q. Obaid, Development of gas sensors for NO2 and H2S gases using selenium nanoparticles prepared by the plasma jet system, *J. Theoret. Appl. Phys.* 18 (2024) 1–8, <https://doi.org/10.57647/j.jtap.2024.1806.73>.
- [49] N.A. Kamaruzaman, A.R. Yusoff, N.A. Malek, M. Talib, Fabrication, characterization and degradation of electrospun poly (ε-caprolactone) infused with selenium nanoparticles, *Malays. J. Fundam. Appl. Sci.* 17 (2021) 295–305.
- [50] S. Menon, H. Agarwal, S. Rajeshkumar, P.J. Rosy, V.K. Shanmugam, Investigating the antimicrobial activities of the biosynthesized selenium nanoparticles and its statistical analysis, *Bionanoscience* 10 (2020) 122–135, <https://doi.org/10.1007/s12668-019-00710-3>.
- [51] T. Deepa, S. Mohan, P. Manimaran, A crucial role of selenium nanoparticles for future perspectives, *Results. Chem.* 4 (2022) 100367, <https://doi.org/10.1016/j.rechem.2022.100367>.
- [52] S. Vasanthakumar, M. Manikandan, M. Arumugam, Green synthesis, characterization and functional validation of bio-transformed selenium nanoparticles, *Biochem. Biophys. Rep.* 39 (2024) 101760, <https://doi.org/10.1016/j.bbrep.2024.101760>.
- [53] D. Ravi, B. Gunasekar, V. Kaliaperumal, S. Babu, A Recent Advances in Antimicrobial Activity of Green Synthesized Selenium Nanoparticle, *Open Nano* (2024) 100219, <https://doi.org/10.1016/j.onano.2024.100219>.
- [54] B.R. Alsehli, M.F. Al-Hakkani, A.H. Alluhayb, S.M. Saleh, H. Mohamed, A. M. Hassane, M.H. Hassan, Facile Mycosynthesis of Selenium Nanoparticles by *Aspergillus candidus* Extract: unveiling Characterization, Potent Antimicrobial Properties, and Cytotoxic Activities, *Bionanoscience* 15 (2) (2025) 234, <https://doi.org/10.1007/s12668-025-01845-2>. Jun.